FINAL REPORT

ON

INVESTIGATION INTO THE PERFORMANCE OF ALUMINUM WOUND DISTRIBUTION TRANSFORMERS

Indian Institute of Technology Roorkee
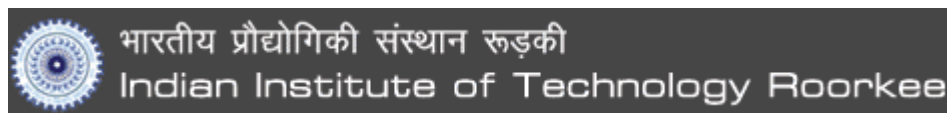
Investigators

Prof. H. O. Gupta

Department of Electrical Engineering
Indian Institute of Technology Roorkee
ROORKEE – 247 667
Email ID: harifee@iitr.ernet.in

Dr. D. K. Dwivedi

Associate Professor
Mechanical and Industrial Engg. Dept.
Indian Institute of Technology Roorkee
ROORKEE – 247 667
E mail ID: dkd04fme@iitr.ernet.in

ACKNOWLEDGMENT

OBJECTIVE

The stresses responsible for transformer failures, creep behavior of aluminum conductor, operating conditions, frequent magnetic inrush current and their effects on the life of distribution transformer (DTs) are being investigated. It is being investigated by conducting experiments that hot spot temperature, creep behavior of aluminum conductor, and frequent switching of DTs in the field may be responsible for excessive failures. This is due to the fact that winding conductors between spacers become loose due to elongation which in turn causes turn to turn fault in the winding. The steady state creep rate is an important design parameter which specifies strain rate in the wire during steady state creep stage. By accomplishing experimental work, the steady state creep rate is calculated and presented for aluminum and copper wire of 0.8 and 0.62 mm, respectively at various temperature and stress conditions. By taking this parameter into account, dependence of aluminum and copper on temperature and stress are presented. The temperature for creep tests are taken 100 °C and 140 °C corresponding to hot spot temperature conditions. The stresses for creep tests are calculated between 1.24 kg/mm^2 and 6.64 kg/mm^2 corresponding to different values of inrush current. A comparison of steady state creep rate of aluminum and copper wires is also presented at same temperature and stress conditions. The loss of life for 25, 63 and 100 kVA DTs, due to inrush current and cold load pick up (CLPU) condition is also presented in this report. Based on experimental findings recommendations and suggestions have been made for procuring reliable aluminum and copper wound DTs.

The project could not be completed within the stipulated time due to late delivery and installation of creep testing machine which was fabricated specially as per our need. The experimental work is being carried out and data being collected.

CONTENTS

LIST OF FIGURES

LIST OF PHOTOGRAPHS

LIST OF TABLES

LIST OF ABBREVIATIONS

CLPU   Cold Load Pick UP

DTs   Distribution Transformers

FESEM   Field Emission Scanning Electron Microscopy

HST   Hot Spot Temperature

IR   Inrush Current

LOL   Loss of Life

SEM   Scanning Electron Microscopy

INVESTIGATION INTO THE PERFORMANCE OF ALUMINUM WOUND DISTRIBUTION TRANSFORMERS

1. INTRODUCTION

In India, yearly failure rate of distribution transformers (DTs) are in the range of 15% to 25% as against 3 to 5% in Western countries. The major reasons for the failure of DTs are thermal, electrical and mechanical stresses on transformer winding insulation. The life of DTs is normally gauged from the life of its insulation in proximity of Hot Spot Temperature (HST). The insulation deterioration due to thermal stresses is slow but continuous [1-3] and may be high during cold load pick up (CLPU) [7], due to electrical stresses the deterioration occurs where field intensity becomes more than a particular value and it is very fast [1,2]. Mechanical stresses due to short circuit and switching inrush current play a major role in the deterioration of transformer winding insulation.

In India most of the utilities have frequent tripping due to demand exceeding generation, and poorly maintained distribution lines. Thus, repeated switching of the transformers take place causing CLPU and the transient magnetic inrush current. This inrush current may be as high as 10 times or more of rated current and persists only for about one half of a second. Inrush current peak of equal or more than 60% of the rated short circuit current cause local forces of the order of magnitude as those during short circuit and hence similar damage to the winding that may be due to short circuit [4]. This current produces excessive mechanical stress and intense localized heating which may be sufficient to cause elongation of aluminum conductor may be due to creep. Inrush currents which produce forces in order of the short circuit forces cause large damage on the winding as it occurs more frequently than that of the short circuit current (as switching is more in India) and with a significant longer duration [5]. Thus at every occurrence of the inrush, there is some degradation of aluminum conductor and its insulation. After many such inrushes local heating may take place in the winding causing ultimate failure of the transformer.

Restoration of power distribution network after a prolonged interruption produces a load demand significantly higher in magnitude and different behavior than pre-interruption condition. It can be categorized in four phases based on magnitude and nature of the current. These phases are inrush, motor starting, motor running, and enduring phase. In first inrush phase the current magnitude rise up to 10 to 15 times the pre-outage value for few cycles. It is mainly because of magnetization of DTs; however, the starting current of cold lamp filament also has minor effect. In the second phase, the magnitude of the current increases up to 6 times the normal value due staring current of motors and this phase sustain for about a second. The third phase causes because of the increased current required for acceleration of motors and it lasts for about 15 seconds. These three

phases may cause excessive mechanical stress to degrade the winding insulation. The fourth phase is due to the loss of diversity among the thermostatically controlled loads and it continues until the normal diversity amongst the loads is restored. The duration varies from few minutes to hours depending upon various factors such as weather, nature of load, duration of interruption etc. The load current magnitude in this enduring phase may be nearly 2 times of the normal load [7]. This phase causes high HST in the windings of the transformers and thereby accelerated loss of life of the winding insulation. CLPU problem is being observed by Indian utilities in some localities.

The literature survey revealed that, not much attention has been paid to estimate the probability of failure of DTs subjected to very frequent switching which leads to the occurrence of Inrush currents and CLPU problem. It is envisaged that excessive failure rate of aluminum wound DTs may be due to this phenomenon. Also CLPU, thermally degrade the insulation of the windings. It is therefore, attempts were made to evaluate the effect of inrush current and CLPU on the failure tendency of DTs. Other reasons of failures of DTs are discussed in detail in the earlier publications of Gupta [8] and first interim report of the project.

2.   COMPUTATION OF LOSS OF LIFE

The loss of life estimation depends on the parameters affecting the service life. Transformer operation at high temperature causes reduced mechanical strength of both conductor and structural insulation. These effects are of major concern during periods of transient over current like inrush conditions or short circuit conditions (through-fault) when mechanical forces reach their highest levels and occurrence CLPU problem. An algorithm has been presented in the section 2.1 and 2.2 below for computing the loss of life of DTs of the given rating due to Inrush current and CLPU, respectively.

2.1. COMPUTATION OF LOSS OF LIFE DUE TO INRUSH CURRENT

2.1.1. INRUSH CURRENT

Poor generation and load shedding cause repeated tripping of poorly maintained distribution lines. Thus repeated switching of transformers takes place. Every time when a transformer is energized a transient current much larger than the rated transformer current can flow for several cycles. This is caused because the transformer will always have some residual flux density and when the transformer is re-energized the incoming flux will add to the already existing flux which will cause the transformer to move into saturation. This transient current may be as high as ten or more times the full- load current and persists for a short duration (about one-half second). This transient current is known as Inrush Current. Though this current persists only for a short duration but repeated currents causes production of excessive mechanical stresses, intense localized

heating or hot spot temperature of the windings which eventually leads to damage of insulation, and voltage drop at the consumer's end.

The peak value of the inrush current [6] can be estimated under saturated conditions by the equation (1) as follows:

$$i_{rmax} = \frac{\sqrt{2}V}{\sqrt{(\omega L_{air})^2 + R_{dc}^2}} \left(\frac{2B_m \cos\alpha + B_{res} - B_{sat}}{B_m} \right)$$ (1)

where,
V = Applied Voltage (Volts)
L_{air} = Air core inductance of the DT (Henry)
R_{dc} = DC resistance of the transformer windings (Ohms)
B_m = Peak value of induction in iron at the moment of switching (Tesla)
B_{res} = Residual flux density of core material (B_{res} =0.83* B_m Tesla)
B_{sat} = Saturation flux density of core material (B_{sat} =1.9 Tesla)
α = Switching angle (degrees)

2.1.2. ALGORITHM

Step 1: COMPUTATION OF SHORT CIRCUIT CURRENTS AND THRESHOLD VALUE

Compute the short circuit current i_{sc} for DTs of the given rating using (2) and threshold value i_{th} using (3) as follows:

$$i_{sc} = k\sqrt{2}\frac{i_{phase}}{Z_{pu}} \times 100$$ (2)

$$i_{th} = 0.6 \times i_{sc}$$ (3)

Where
$k\sqrt{2}$ = Asymmetric factor whose value is decided based on X/R ratio with reference to IS:2026, Part-1-1977 Clause 16.11.2
i_{phase} = Phase current of the transformer (Amp)
Z_{pu}= per unit Impedance

Step 2: COMPUTATION OF PROBABILITY OF INRUSH CURRENT MORE THAN THRESHOLD VALUE i_{th}

(a) For B_r (residual flux) values varying between 0 to nB_{max} (n is the maximum percentage   value) in steps of m repeat the following steps:
   i) Compute peak value of inrush current, for each switching angle (0 to 360 deg)   using (1).
   ii) Compute the current ratio (peaks of inrush current to the short circuit current) for each switching angle.

$$Current\ Ratio = \frac{i_{r\,max}(\alpha)}{i_{sc}} \tag{4}$$

where α =Switching angle $[0 \le \alpha \le 360^O]$

iii) Find the number of switching angles, for which the inrush current is greater than the threshold value i_{th}. Let r =Total no. of angles at which $i_{rmax} \ge i_{th}$.

iv) Compute the probability of switch on causing deterioration of windings (p_d) for the residual flux B_r

$$p_d(B_r) = \frac{r}{360} \tag{5}$$

(b) Calculate the probability of switch on causing $i_{rmax} \ge i_{th}$

$$P(i_{rmax} \ge i_{th}) = \frac{\sum pdanger}{m} \tag{6}$$

Step 3: COMPUTATION OF MECHANICAL STRESSES

When the inrush current becomes equal or greater than the threshold value, the mechanical stresses developed due to inrush current are same as that during the short circuit current. The mechanical stresses for two winding, three phase transformer having a core type construction and concentric winding with tapings placed within the body of the outer winding is calculated as

a. CALCULATE HOOP STRESS (σ_{mean})

Hoop stress is a mechanical stress acting circumferentially (perpendicular both to the axis and to the radius).

$$\text{Hoop stress}\,(\sigma_{mean}) = K\frac{I_{ph}^2 R_{dc}}{h_w Z_{pu}^2}\ \text{kg/cm}^2 \tag{7}$$

where

$$K(Al) = 0.02\left(\frac{k\sqrt{2}}{2.55}\right)^2$$

h_w = winding height (mm)

The value of $k\sqrt{2}$ is obtained from step (1). The obtained value of hoop stress shall be less than 700 kg/cm^2 for aluminum.

b. CALCULATE RADIAL BURSTING FORCE (F_r)

These forces tend to increase the distance between the windings and causes damage to the windings.

$$\text{Radial bursting force } (F_r) = \frac{2\pi\sigma_{mean}I_{ph}N}{\delta} \quad \text{kg} \tag{8}$$

where,

δ = Current density [Amps/mm^2]

c. CALCULATE INTERNAL AXIAL FORCE (F_c):

Axial forces bend the winding turns in a vertical direction. These forces also increase the pressure acting on spacers between coils.

$$F_c = (-)\frac{34S_n}{Z_{pu}h_w} \quad \text{Kg} \tag{9}$$

where,

S_n = Rating of the transformer (KVA)

The negative sign indicates that force is acting towards the center

d. CALCULATE MAXIMUM COMPRESSIVE PRESSURE IN THE RADIAL SPACERS (P):

The one-third of the internal axial force (Fc) exerts on the outer windings of DTs. Therefore the compressive force on the windings is

$$P = \frac{F_c}{3 \times A} \quad \text{(kg/cm}^2\text{)} \tag{10}$$

where,

A=Total supported area of the radial spacer (cm^2)

e. CALCULATE THE RESULTANT FORCE ON THE CONDUCTOR JUST BELOW/ABOVE THE SPACERS

The maximum value of the hoop stress is two times of the mean value and it is on the inner layer of the outer windings. Therefore, the resultant stress on the conductor just below/above the radial spacer of the inner layer of most stressed coil is given as follows:

$$\text{Resultant Stress in kg/cm}^2 = \sqrt{(2 \times \sigma_{means})^2 + (P+40)^2} \tag{11}$$

where, 40 Kg/cm^2 is the tightening force taken into account.

Step 4: COMPUTATION OF LOSS OF LIFE (LOL) PER SWITCHING

Compute loss of life per switching taking into account the failure statistics of the DTs.

$$LOL \text{ per Switching} = \frac{Yearly \text{ Failure Rate on account of Switching}}{No. \text{ of Switch on per Year}} \tag{12}$$

Step 5: COMPUTATION OF LOSS OF LIFE DUE TO INRUSH GREATER THAN THE THRESHOLD VALUE

Calculate the loss of life due to inrush current using step (2) and step (4)

$$LOL\ due\ to\ Inrush\ Current = \frac{LOL\ per\ Switching}{P(\ i_{rmax}\ \geq\ i_{th}\ )} \qquad (13)$$

2.1.3. RESULTS

For analysis purpose, data from four aluminium wound DTs of Uttar Pradesh and Punjab with rating 11000/433V, 100kVA, 63kVA, 25kVA is collected and is given in Appendix. The maximum value of the residual flux density for CRGO grade M4 used in the considered DTs is 83% of the maximum flux density. Consider the residual flux density values varying from 0 to $0.83B_{max}$ (n=0.83) in steps of 0.01 (m=84) and various switching ranging from 0 to 360 degrees, the peak value of inrush current is calculated using step 2 for the considered DTs. The calculated maximum inrush current (peaks) at zero switching angle with different residual flux density is shown in Fig.1 for all considered DTs.

Figure 1 shows that for low rating DTs, the probability of occurrence of inrush current greater than the threshold value is at every residual flux density compared to the high rating DTs. Therefore, for low rating DTs, if the number of switching per day is more at zero switching angles, the occurrence of inrush current peaks is not safe for the DT for all values of residual flux density.
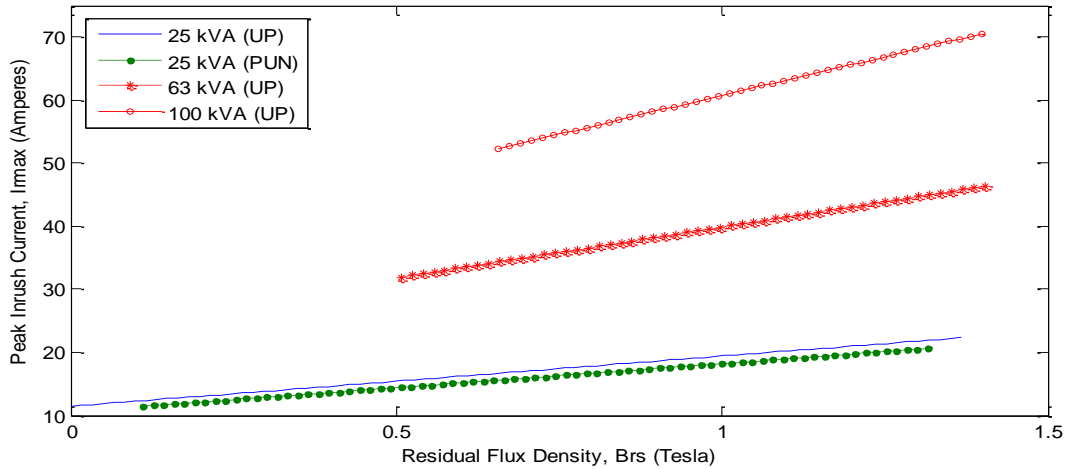
Fig.1. Peak Inrush Current (i_{rmax}) vs. Residual Flux Density (B_r)

The probability of switch on causing deterioration of the winding, for different current ratios (i_{rmax} /i_{sc}) as explained in step 4 is calculated. The calculated probability with residual flux density is shown in Figure 2, 3, 4 & 5 for the considered DTs. It can be clearly seen from the figures that for low rating DTs, the danger of the deterioration of the windings is more than for high rating DTs. As the rating of the DT is increasing, the effect of the inrush current is decreasing. This may be the reason for the failure of low rating DTs is more than high rating DTs.
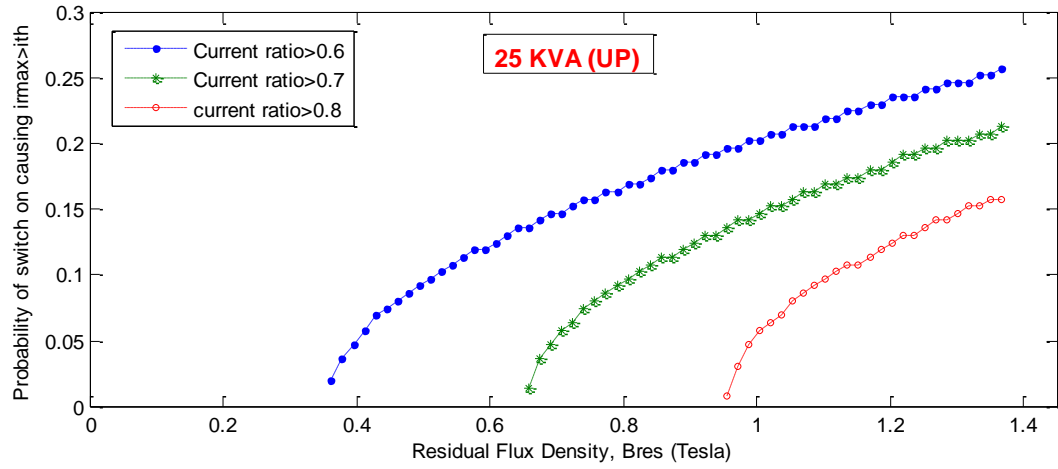
Fig. 2. P(i$_{rmax}$>i$_{th}$) vs. B$_r$ for 25kVA DT (UP)
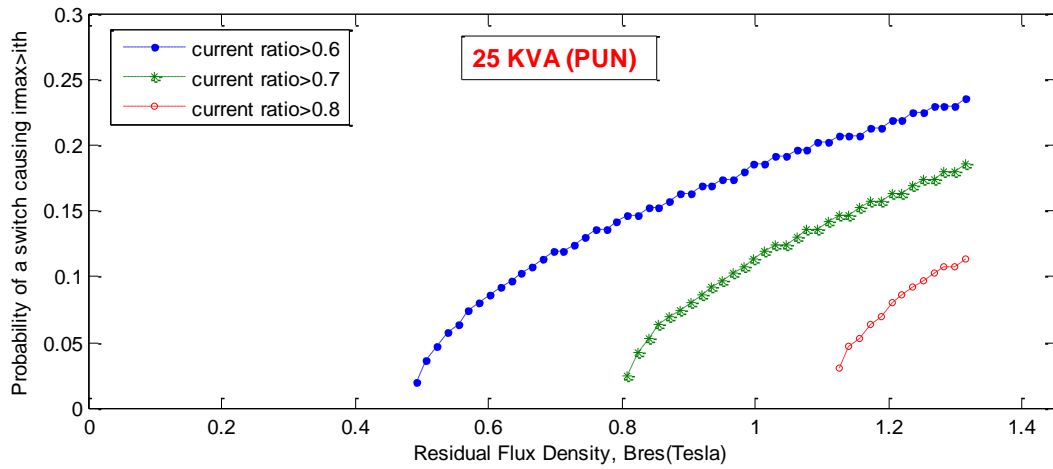
Fig. 3. P(i$_{rmax}$>i$_{th}$) vs. B$_r$ for 25kVA DT (Punjab)
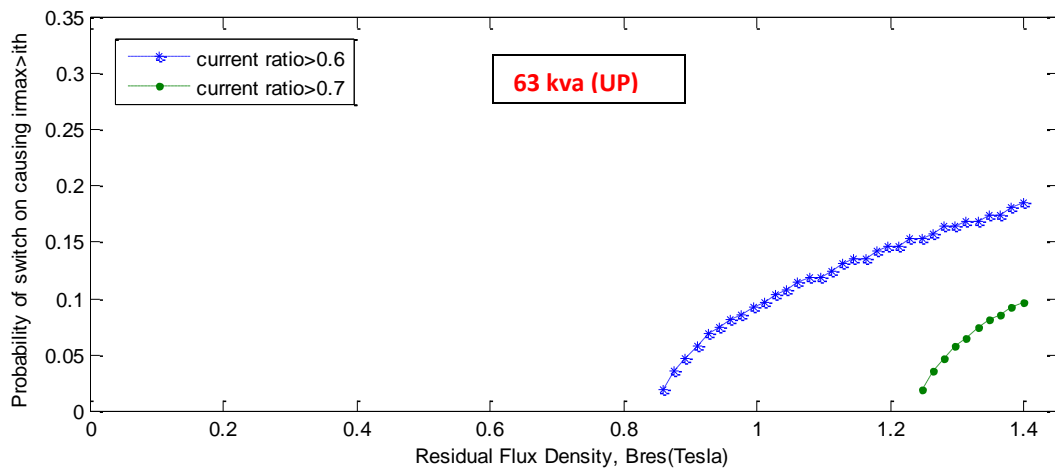
Figure 4. P(i$_{rmax}$>i$_{th}$) vs. B$_r$ for 63kVA DT (UP)
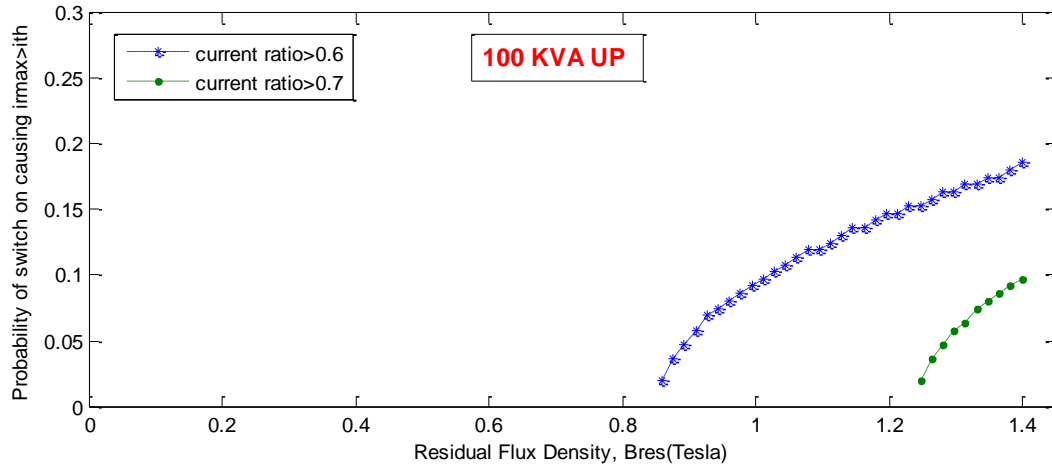
Figure 5. . P(i_{rmax}>i_{th}) vs. B_r for 100kVA DT (UP)

Now assuming one switching per day and failure rate of aluminum wound DTs as 15% on account of inrush, the failure probability of DT per switching is found to be .000411. The probability of dangerous switch on causing $i_{rmax} \geq i_{th}$ is calculated using step 2 for DTs considered and is shown in Table 1.

The loss of life of DTs due to the peak inrush current is calculated using step 4 and is given in Table 2. The mechanical stresses developed due to short circuit current have been calculated. These stresses are the same when the inrush current becomes greater than the 60% of the short circuit current. The calculated mechanical stresses developed on the primary windings for the considered DTs is given in Table 3 and Table 4 respectively.

Table 1: Probability of switch on causing i_{rmax}>=i_{th}

Particulars (KVA)		Probability of switch on causing i_{rmax}>=i_{th}		
		i_{rmax} /i_{sc} >=0.6	i_{rmax} /i_{sc} >=0.7	i_{rmax} /i_{sc} >=0.8
UP	100	0.0768	0.0296	0.0012
	63	0.1007	0.0507	0.014
	25	0.1253	0.0739	0.0329
PUN	25	0.0984	0.0486	0.0125

Table 2: Loss of life of DTs due to inrush current

Particulars (KVA)		Loss of life of DTs		
		i_{rmax} /i_{sc} >=0.6	i_{rmax} /i_{sc} >=0.7	i_{rmax} /i_{sc} >=0.8
UP	100	0.0054	0.0139	0.3425
	63	0.0041	0.0081	0.0293
	25	0.0027	0.0027	0.0039
PUN	25	0.0023	0.0033	0.0051

Table 3: Calculated mechanical stresses during short circuit on HV windings of DTs

Particular	UP			PUN
KVA	100	63	25	25
B_{max} (Tesla)	1.685	1.69	1.647	1.585
σ_{men} (kg/cm^2)	110.8	77.7	40.67	43.84
F_r (kg)	53466.6	33214.4	10464.2	11417.98
F_c (kg)	1757.28	1175	517.3	556.3
P (kg/cm^2)	9.039	6.089	3.454	3.419

Table 4: Calculated stress on the most stressed conductor of HV windings of DTs

Particulars	UP			PUN
Stress (Kg/cm^2)	100	63	25	25
Hoop Stress	110.8	77.7	40.67	43.84
Compression Stress	9.039	6.089	3.454	3.419
Resultant Stress	270.64	201.49	124.79	131.1

2.2. COMPUTATION OF LOSS OF LIFE DUE TO COLD LOAD PICK UP

2.2.1. CLPU

CLPU is the most severe non fault condition faced by the utilities. This problem occurs where the power outages are very frequent. The thermostatically controlled loads such as electric space cooling/heating devices and industrial illumination are major factors for CLPU problem. Fig.6 shows typical load during CLPU. During the time ΔT, the load increases to many times the normal load because of the loss of diversity during this time.. The later phase shows the enduring behaviour and takes hours to settle and the steady state phase.
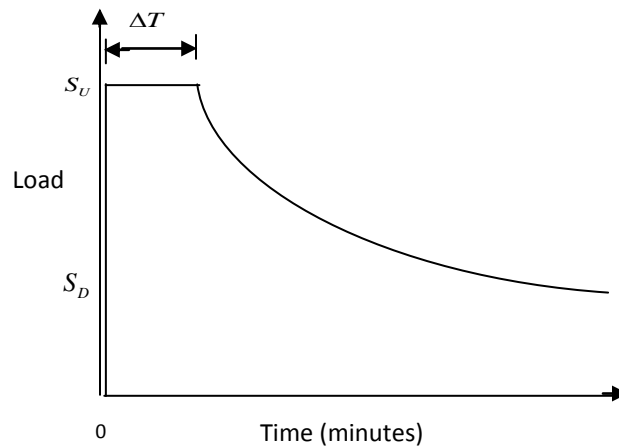
Fig. 6 Load during CLPU

The load during period ΔT is about 1.5 to 2.5 times of the normal load in the developed countries due to large thermostatically controlled load and the load are switched on in a controlled manner to reduced excessive loading on the transformer during CLPU. For Indian environment, this may be taken as 1.5 to 2 times of the normal load but there is no provision to switch on the loads in a controlled manner to overcome CLPU problem. The CLPU problem occurs very frequently in Indian utilities causing excessive degradation of the winding insulation near winding HST.

2.2.2. ALGORITHM

With typical values of the loadings on the DTs, HST and loss of life during CLPU is calculated by the procedure presented as below:

i)   Compute Factor for load loss (k) = $(\dfrac{Load\ on\ the\ Transformer}{Rated\ Load\ on\ the\ Transformer})^2$

ii) Total loss at rated load = no load loss + load loss

iii) Total loss during time ΔT = (k× load loss) + no load loss

iv) Compute $L = (\dfrac{Total\ loss\ during\ time\ \Delta T}{Rated\ total\ loss\ of\ the\ Transformer})$

v) The winding temperature rise at end of ΔT minutes after switch on,

$$\theta_T = (1 - e^{-\frac{\Delta T}{\tau_w}}) \times \theta_w \times L$$

   where, τ_w = Thermal time constant of windings

   θ_w = Winding temperature rise of rated load

vi) Winding Temperature $\theta_{WT} = \theta_w + \theta_{amb}$

   Where θ_{amb} = Ambient temperature

vii) Calculated HST at time ΔT, $\theta'_{HOT} \approx 1.2 \times \theta_T + \theta_{amb}$

viii) HST at rated load, $\theta_{HOT} \approx 1.2 \times \theta_w + \theta_{amb}$

ix) Rate of loss [3] of life at $\theta'_{HOT} = \dfrac{\Delta T}{t_0} e^{\alpha(\theta'_{HOT} - \theta_{HOT})}$

   Where $\alpha = 0.0865$, $t_0 = 24 \times 60$ minutes

2.2.3. RESULTS

Considering the load during CLPU fourth phase time of 30 minutes (ΔT =30 minutes) as 2 times (i.e. n=2), the average winding temperature rise (θ_w) as 50⁰C and ambient temperature as 35⁰C, HST is calculated at the end of time ΔT and Rate of loss of life and is given in Table 5. The thermal time constant of the windings is taken as 15 minute. The loss of life during this period ΔT is equivalent 4.6 to 5.76 days and HST may touch

as high as 160˚c. Due this phenomenon high failure rate DTs has been reported in some areas of India and likely to be more severe in due course of time.

Table 5: Calculated loss of life due to CLPU problem

| Particulars	Total loss at rated Load (W)	Total loss during Time ΔT (W)	$\theta^{'}_{HOT}$ (^{0}C)	loss of life at $\theta^{'}_{HOT}$ in days
100	1940	4685.6	160	5.76
63	1415	3341.6	157.4	4.6
25	785	1853.6	157.4	4.6
25	770	1838.6	158.8	5.2

3.   EXPERIMENTAL RESULTS

This section describes the metallography, chemical composition, tensile properties at room temperature and elevated temperatures and creep behaviors of aluminium wires with and without flow of current under different stress and temperature conditions. The samples were taken from the windings of different DTs of different ratings. The mechanical and metallurgical studies have been performed on the aluminium specimens.

3.1.   METALLOGRAPHY

The micrographs of Aluminium specimens were different magnifications (Fig. 6). The metallographic examination of specimens revealed a microstructure that consisted of some traces of impurities with the Aluminium matrix. The presence of the second phase (grey) indicating existence impurities/alloying in the aluminium matrix. From the micrographs, it can be observed that inclusions are present in the base metal. The percentage of these second phase particles was 1-2% except in one sample having 6% of these inclusions as determined with the help of ImageJ software. With the ImageJ software, the analyzed features (inclusions) images of all the specimens had been taken by adjusting the threshold and then by using these features (inclusions) images of the specimens, the total area of the aluminium matrix and the second phase elements was obtained which was used to find the percentage of second phase elements (impurities) present in the aluminium matrix. The Scanning Electron Microscopy (SEM) of aluminum specimen are shown in Fig. 7. The features analyzed (inclusions) using ImageJ for all the specimens are shown in Fig. 8.

Table 6 Chemical Composition of the inclusions aluminium specimen

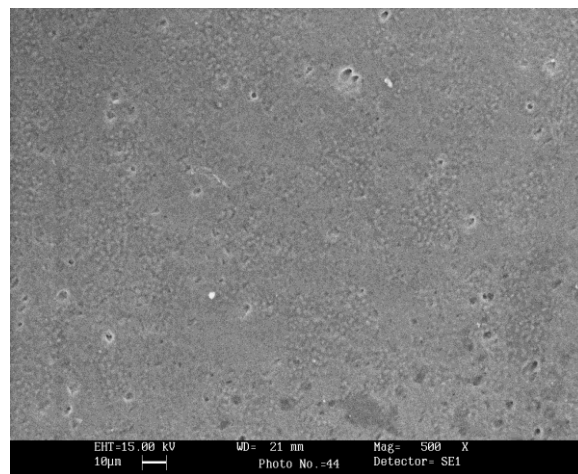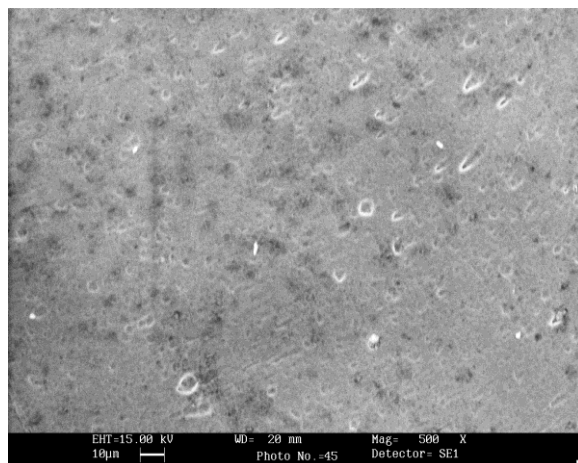| Elements	Wt%
C	03.31
O	00.24
Fe	01.15
Al	95.30
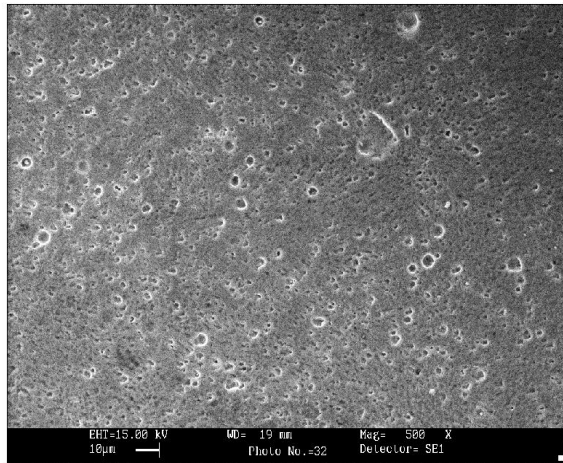
Sample No. -1
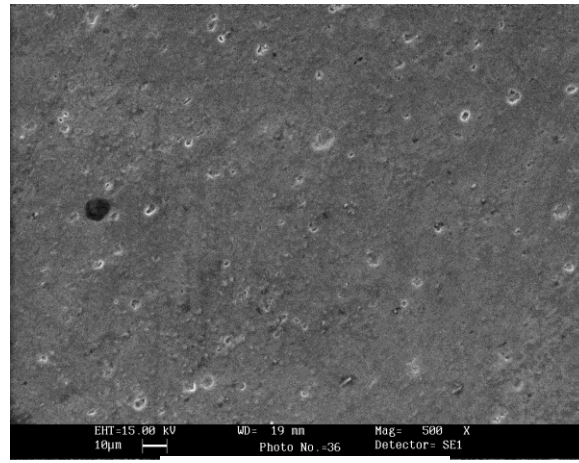
Sample No.- 2
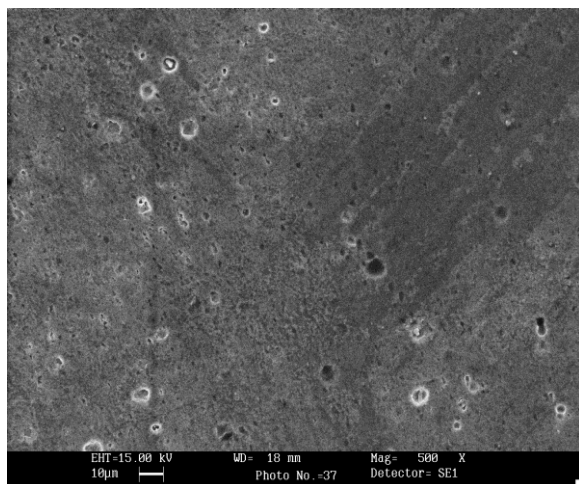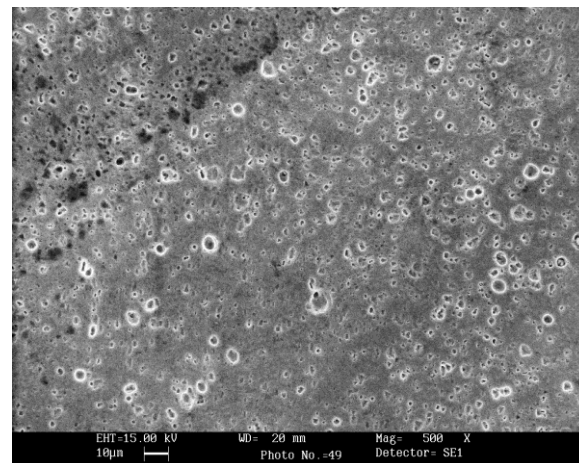

Sample No. -3

Sample No. - 4

Sample No. -5

Sample No. -6

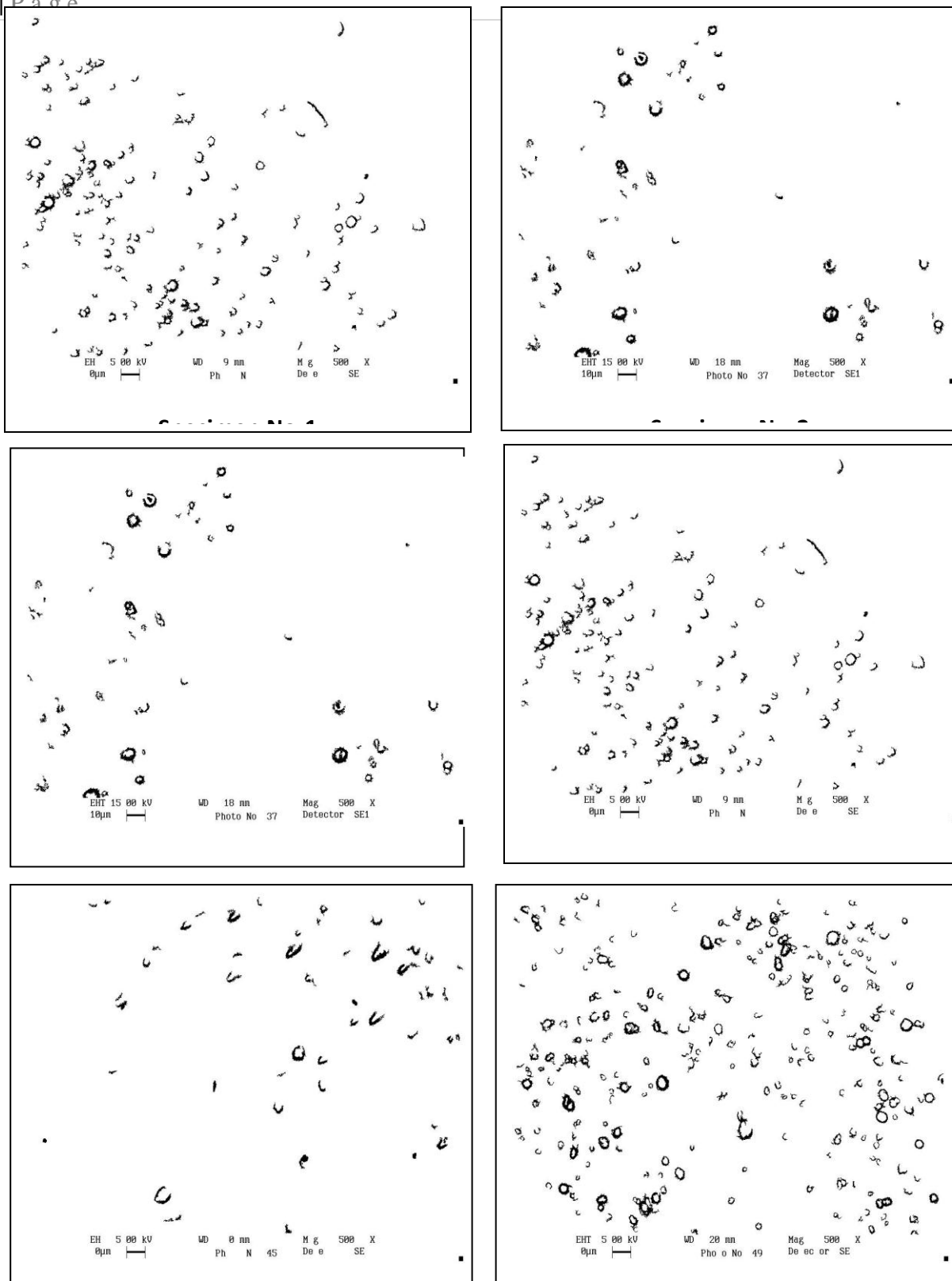Fig.7 SEM images of the aluminium specimens

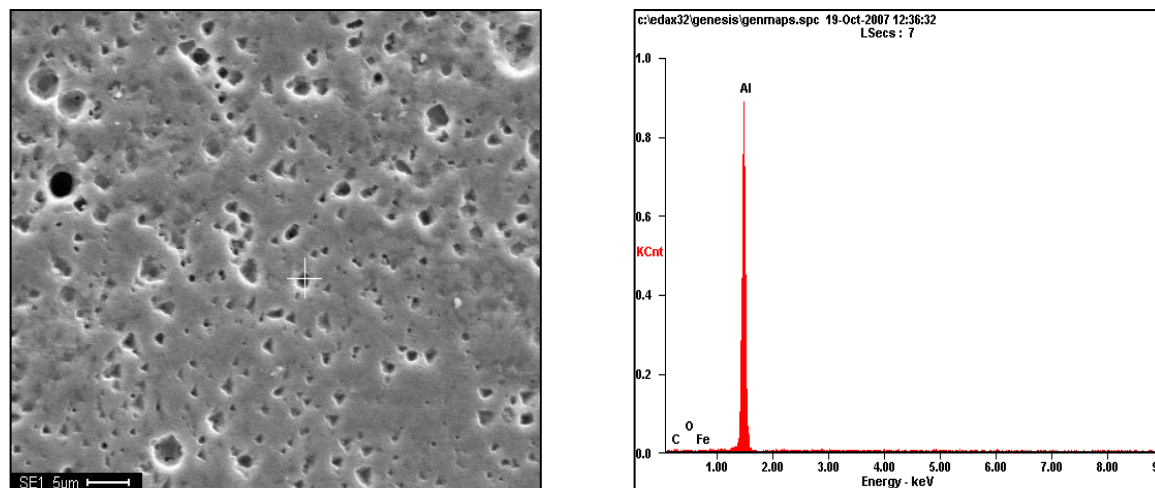Fig. 8 Featured (inclusions only) analyzed using ImageJ software

Fig. 9 FE-SEM results showing the chemical composition of other aluminium specimen

Field emission scanning electron microscope (FE-SEM) showed that these inclusions have carbon, iron and oxygen in aluminium matrix (Fig. 9). Amount of (wt. %) various elements can be seen from Table 6. Presence of these metallic and non-metallic elements is expected to decrease the electrical conductivity and related electrical resistive heating which in turn can affect the creep resistance of aluminium wires used in electrical machinery such as DTs.

3.2. MECHANICAL PROPERTIES

3.2.1. TENSILE TESTING

The mechanical properties of the six samples of aluminium wire tested at different temperatures (room temperature (150^0C). These mechanical properties obtained from tensile test include ultimate tensile strength, yield strength and ductility in terms of %age elongation (Table 7). It can be seen from the Table 7 that an increase in test temperature from 30 to 150^0C, the tensile strength of the Al wire decreases (Fig. 10). Ductility was measured in terms of percentage reduction in area and it was found in the range of 20%-40%. Typical stress-strain curves aluminium sample are shown in Fig. 11. To study the mechanism of the fracture during tensile test fractographs of the tensile fractured surface of the aluminum specimens are analysed by Scanning Electron Microscopy (SEM) as shown in Fig. 12 and was observed that the fracture of almost all the specimen took place in ductile manner which is evident from the presence cuplike depressions called dimples on the fractured surface. These dimples are the result of the microvoids nucleation and coalescence at second phase particle and aluminium matrix. The microvoids nucleate predominantly at particles (inclusions) that are present in the aluminium matrix. After nucleation, the voids grow in the direction perpendicular to the applied tensile stress and secondary voids can also nucleate at smaller particles. During necking, expansion of the voids occurs, leading to the coalescence by void impingement

resulting in higher uniform strain. After failure, a dimpled fracture surface is typically observed.

Table 7 Tensile properties of aluminium wires at different temperatures

Sample No.	Temprature (^{0}C)	Final Diameter (mm)	Ultimate Load (N)	Ultimate Strength (N/ mm^2)	% Reduction
1	25	0.7	70	139.27	23
	50	0.7	70	139.27	23
	100	0.7	60	119.37	23
	150	0.7	50	99.48	23
2	25	0.65	65	129.32	34
	50	0.65	60	119.37	34
	100	0.7	60	119.37	23
	150	0.7	45	89.53	23
3	25	0.6	65	129.32	43
	50	0.65	60	119.37	34
	100	0.6	50	99.48	43
	150	0.7	45	89.53	23
4	25	0.65	65	129.32	34
	50	0.65	60	119.37	34
	100	0.6	55	109.43	43
	150	0.6	50	99.48	43
5	25	0.7	70	139.27	23
	50	0.7	70	139.27	23
	100	0.7	60	119.37	23
	150	0.6	50	99.48	43

6	25	0.6	70	139.27	43
	50	0.7	70	139.27	23
	100	0.6	60	119.37	43
	150	0.7	50	99.48	23
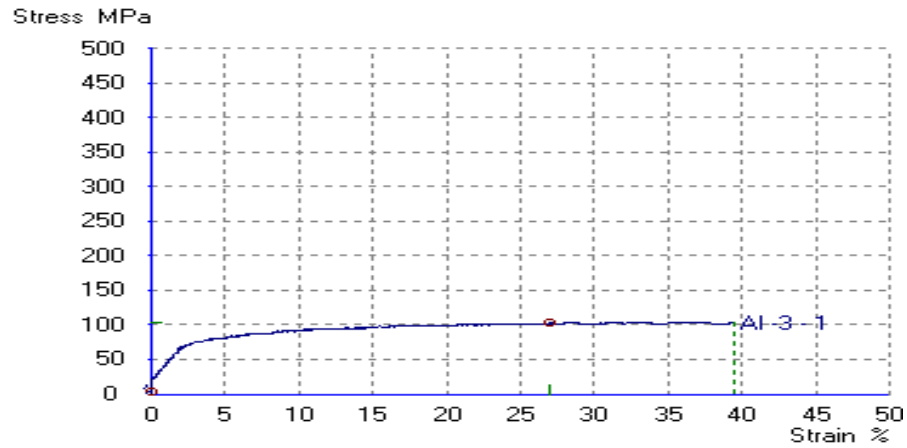
(a)
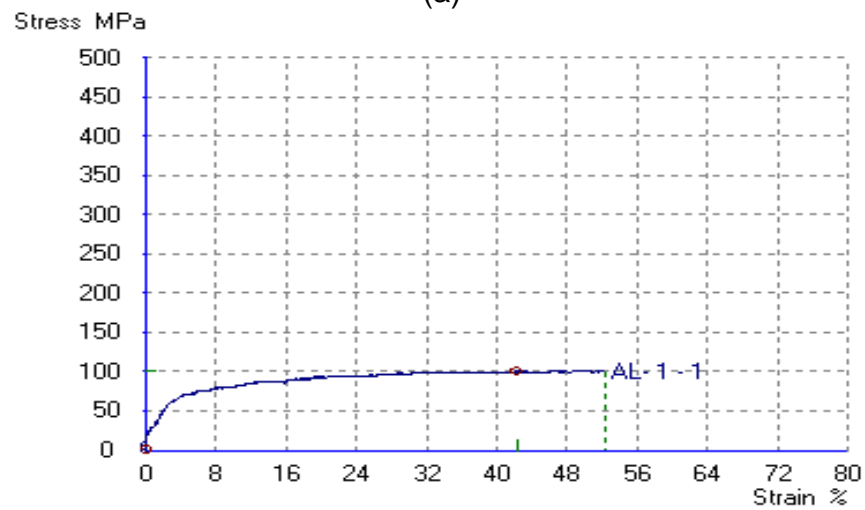
(b)

Fig. 10 Stress vs. strain curves for aluminium specimens.

Fig. 11 Tensile strength vs. temperature relationship for aluminium wires

Specimen No-1

Specimen No-2

Specimen No-3

Specimen No-4

Specimen No-5

Specimen No-6

Fig. 12 SEM fractographs of the tensile fractured surfaces of aluminum specimens

4. CREEP BEHAVIOUR

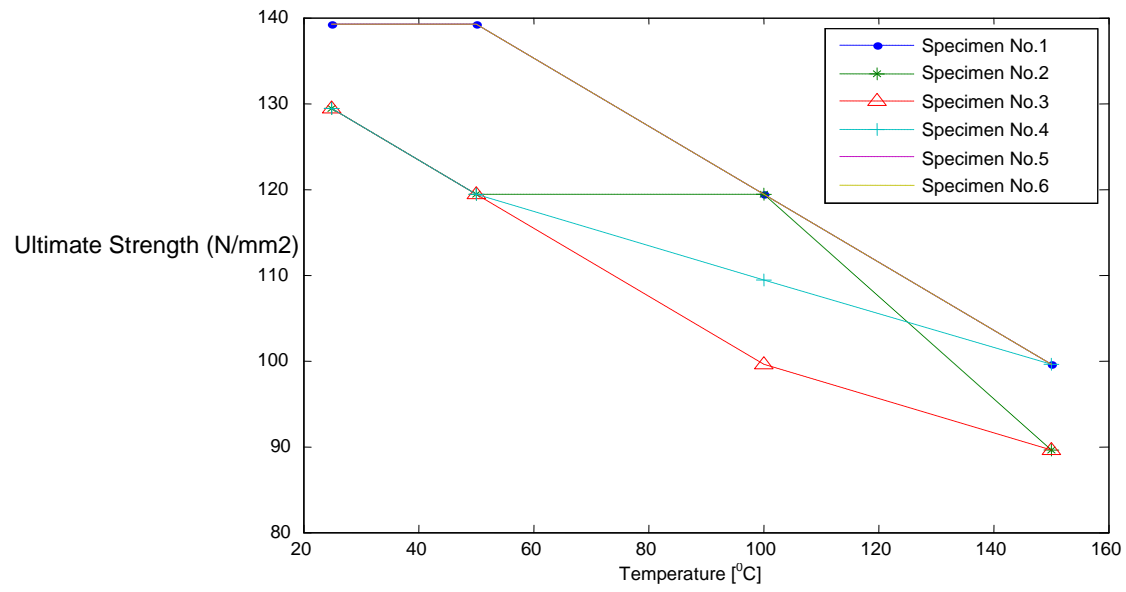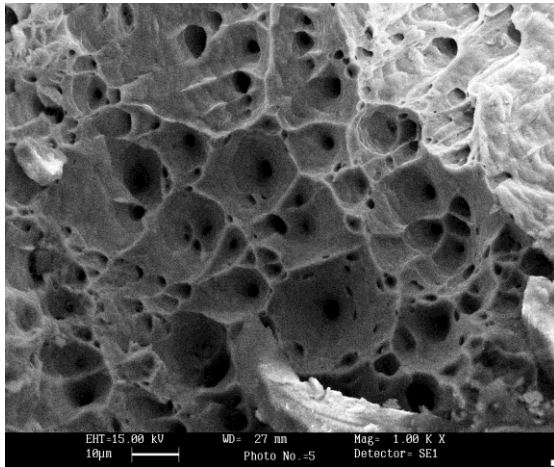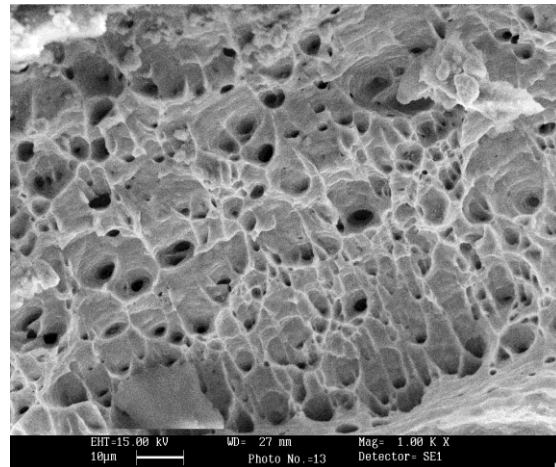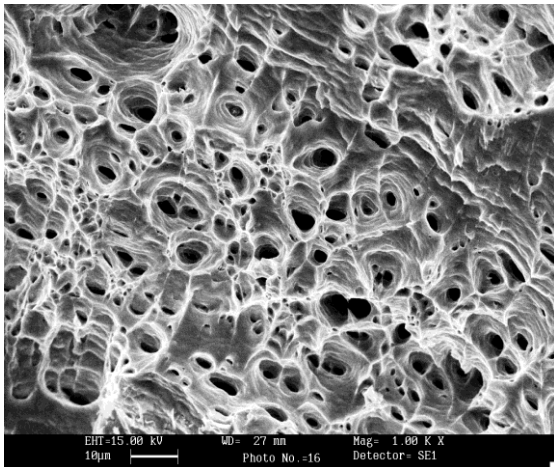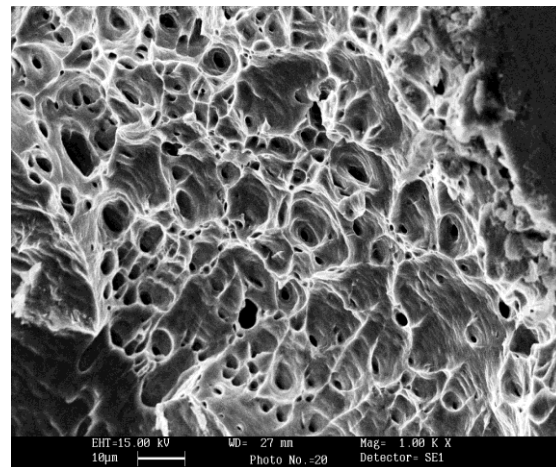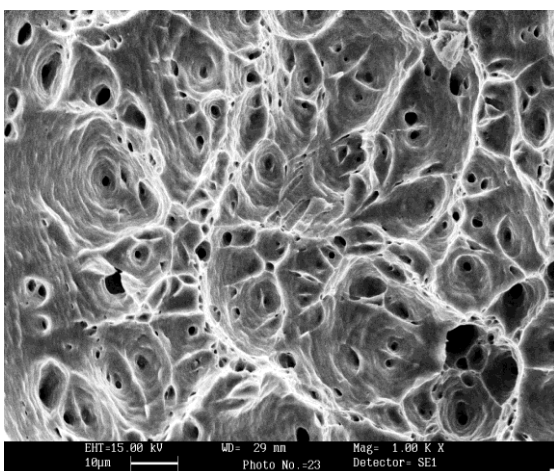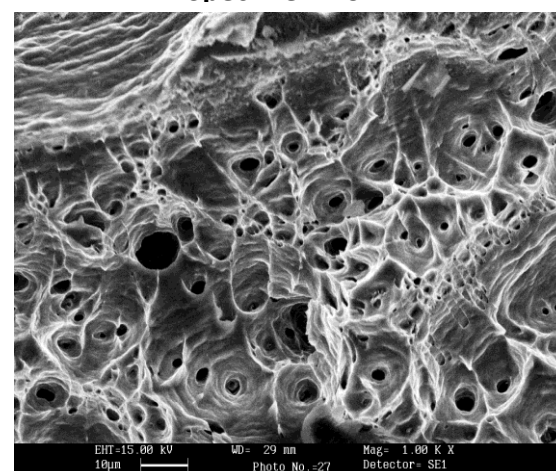Creep behaviour of the aluminium wires under study was investigated without flow current pulses over a range of temperature and stress. The test conditions were selected from the analytical study of electromagnetic forces generated in distribution transformers of different rating.

4.1 CREEP BEHAVIOUR OF Al WIRES WITHOUT FLOW OF CURRENT

Creep behaviour of the aluminium wire (diameter of 0.8mm) at different temperatures and stresses was studied and results of the same have been shown in Fig. 13-15. Creep curve for Al wire tested at 250^0C temperature and 3 kg/mm^2 stress is shown in Fig. 13. It can be observed from the Fig. 13 that an extension of about 1.65mm takes place 140 min of test duration. Analysis of the creep curve showed creep rate of 0.568×10^{-4} mm/mm/min and extension rate of $0.0085\ mm/min$. Creep curve at 150^0C temperature and 3 kg/mm^2 stress is shown in Fig. 14. It can be observed from the Fig. 14 that an extension of about 0.8mm takes place 2500 min of test duration. The creep rate for these conditions is 0.007×10^{-4} mm/mm/min and extension rate is $0.0001\ mm/min$. Creep behaviour of the aluminium wire (diameter of 30.8mm) at higher stresses 5 kg/mm^2 and at 150^0C temperature was studied and results of the same have been shown in Fig. 15. It can be observed from the Fig. 13 that an extension of about 0.9mm takes place 120 min of test duration. Analysis of the creep curve showed creep rate of 0.14×10^{-4} mm/mm/min and extension rate is $.0022\ mm/min$. From the above figures, it has been observed that an increase in temperature from 150^0C to 250^0C at 3 kg/mm^2 stress resulted in a significant increase in creep rate of 0.007×10^{-4} mm/mm/min to 0.568×10^{-4} mm/mm/min. An increase in stress from 3 kg/mm^2 to 5kg/mm^2 at 150^0C temperature the increase in creep rate is 0.007×10^{-4} mm/mm/min to 0.14×10^{-4} mm/mm/min.

Fig. 13 Extension (E) vs. Time (t) relationship for aluminium specimen tested at 250^0C temperature and 3kg/mm^2 stress

Fig. 14 Extension (E) vs. Time (t) Response of Aluminium specimen tested at 150^0C temperature and 3kg/mm^2 stress
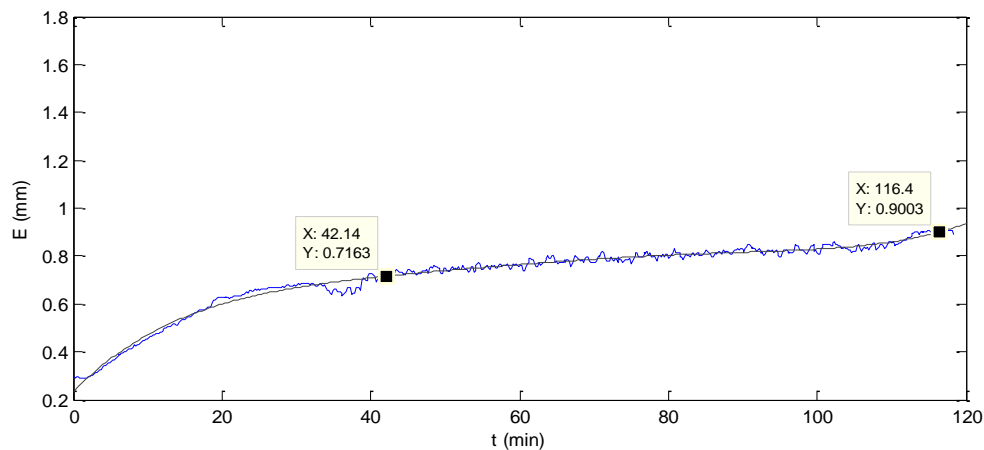
Fig. 15 Extension (E) vs. Time (t) Response of Aluminium specimen tested at 150^0C temperature and 5 kg/mm^2 stress

The creep rupture test of Al wire was conducted at further severe conditions of temperature (300 and 350 ^{0}C) and stress (5.8 kg/mm^2) is shown in Fig. 16-17. Creep rupture conducted at 300 ^{0}C and 5.8 kg/mm^2 shows that an extension of about 16mm takes place in a very short duration 76min and eventually fracture occurs and corresponding creep rates is 3.5×10^{-4} mm/mm/min and extension rate is 0.053 mm/min (Fig. 16). Creep rupture conducted at 350 ^{0}C and 5.8 kg/mm^2 shows that a huge extension of about 14mm takes place in a very short duration 25min and eventually fracture occurs (Fig. 17). It can be seen that the creep rate increases rapidly with the time which is indicating third stage of creep curve. The creep rate is 18×10^{-4} mm/mm/min and extension rate is 0.27 mm/min. From the Fig. 16-17, it can be seen that with the increase in temperature at same stress, the time for the fracture decreases. No clear transition for primary to secondary stage was observed however tertiary stage could be noticed for the creep curve.
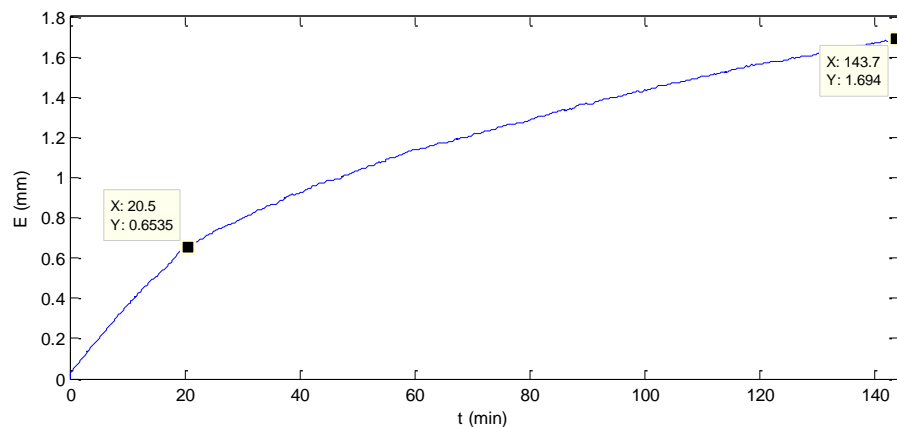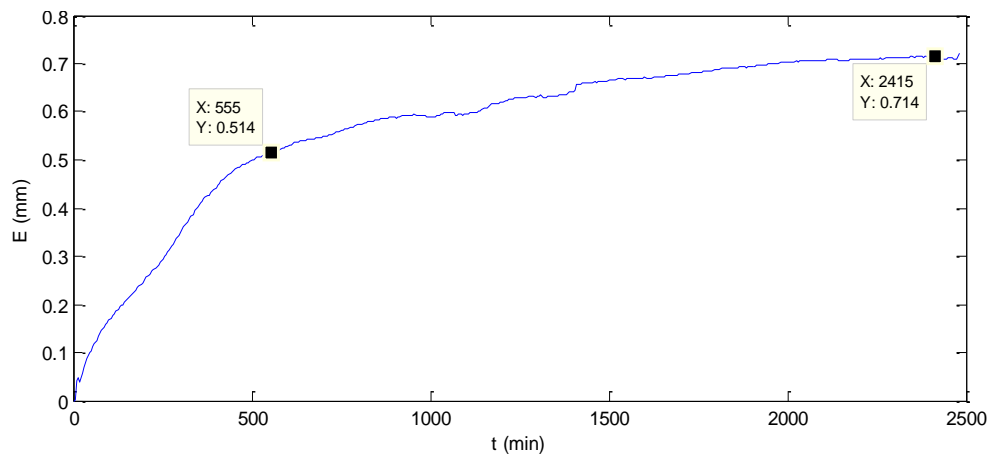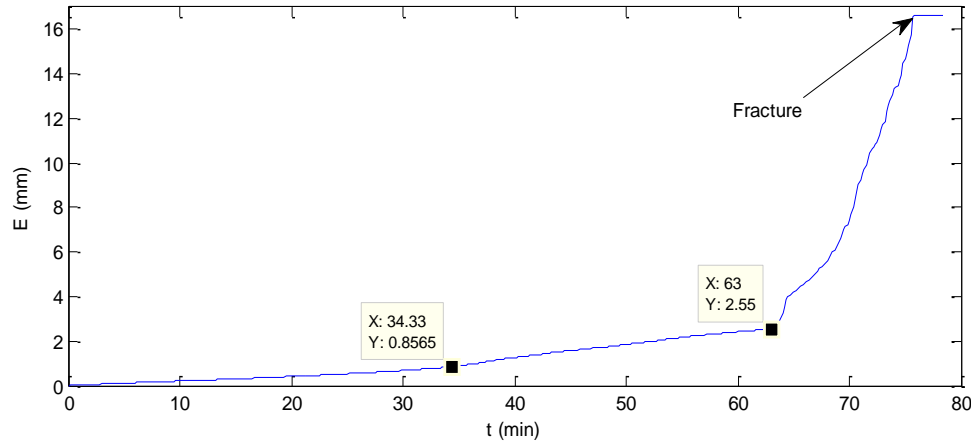
Fig. 16 Extension (E) vs Time (t) Response of Aluminium specimen tested at 300^{0}C temperature and 5.8 kg/mm^2 stress
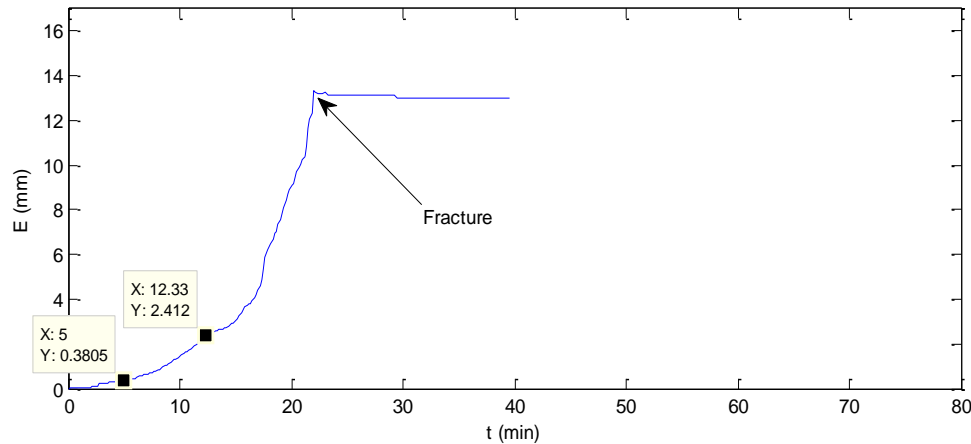
Fig. 17 Extension (E) vs. Time (t) Response of Aluminium specimen tested at 350^{0}C temperature and 5.8 kg/mm^2 stress

4.2. CREEP BEHAVIOUR OF AL WIRE WITH FLOW OF CURRENT

Creep behaviour of the aluminium wire (diameter of 0.8mm) with flow of current at 150^{0}C 3 kg/mm^2 was also studied and results of the same have been shown in Fig. 18-19. Creep of the Al wire under investigation is found to be significantly affected by the pulses of current (range of 5-10A) as creep rate increases manifolds under the effect of flow of current.

The creep curves of aluminium with flow of current (5 and 10A) have been shown in Fig. 18-19. It can be observed from the Fig. 18 that slope of the creep curve increases rapidly with the flow of current (for short duration). Careful observation of data revealed that the a pulse of current 5 A for 2 seconds cause an extension of 70 microns which correspond to creep rate 74×10^{-4} mm/mm/min and extension rate 1.11mm/min. A pulse of 10 A current for about 0.7 seconds cause an extension of 650 microns which correspond to 2.52 mm/min creep rate and 168×10^{-4} mm/mm/min.
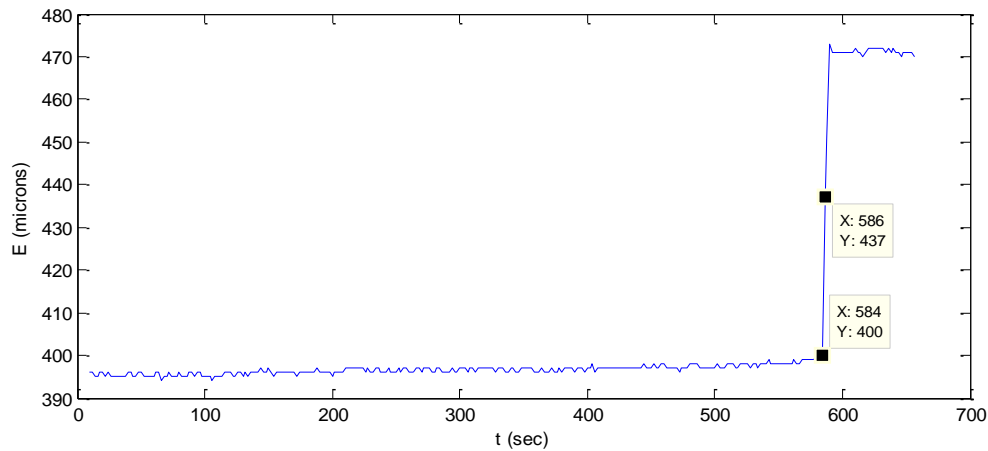
Fig. 18 Extension (E) vs. Time (t) Response of Aluminium specimen tested at 150^0C temperature and 3kg/mm^2 stress with flow of 5A current
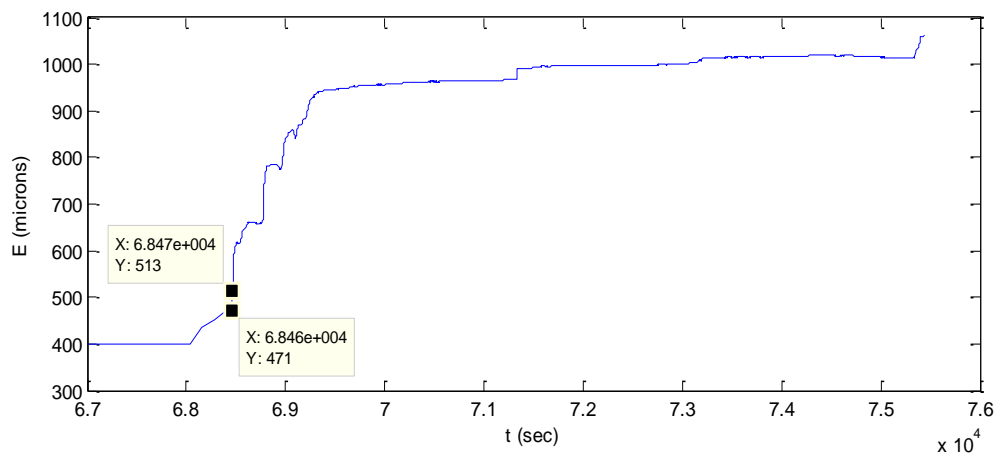
Fig. 19 Extension (E) vs. Time (t) Response of Aluminium specimen tested at 150^0C temperature and 3kg/mm^2 stress with flow of 10A current

Increase in creep rate with flow of current results in excessive electrical resistance heating of thin Al wire which in turn increases the temperature of the wires. The high temperature is known to accelerate the thermally activated mechanisms (diffusional creep, recovery and grain boundary sliding etc.) during creep. These mechanisms soften the material rapidly and decrease the strength of material. This reduction in strength and increase in softness of material at high temperature eventually leads to the high creep rate [10]. This is evident from significant reduction in cross of creep ruptured sample (Fig. 20). The results obtained from the above figures are shown in Table 8.

Table 8 Creep rate for different temperature/stress combinations with and without flow of current

Temperature (^{0}C)	Stress (kg/mm^2)	Without flow of current	
		Strain rate (mm/mm/min)	Extension rate (mm/min)
150	3	0.007×10^{-4}	0.0001
150	5	0.14×10^{-4}	0.0022
250	3	0.568×10^{-4}	0.0085
300	5.8	3.5×10^{-4}	0.053
350	5.8	18×10^{-4}	0.27
		With flow of current	
150	3 + 5A	74×10^{-4}	1.11
150	3 + 10A	168×10^{-4}	2.52

a)   b)
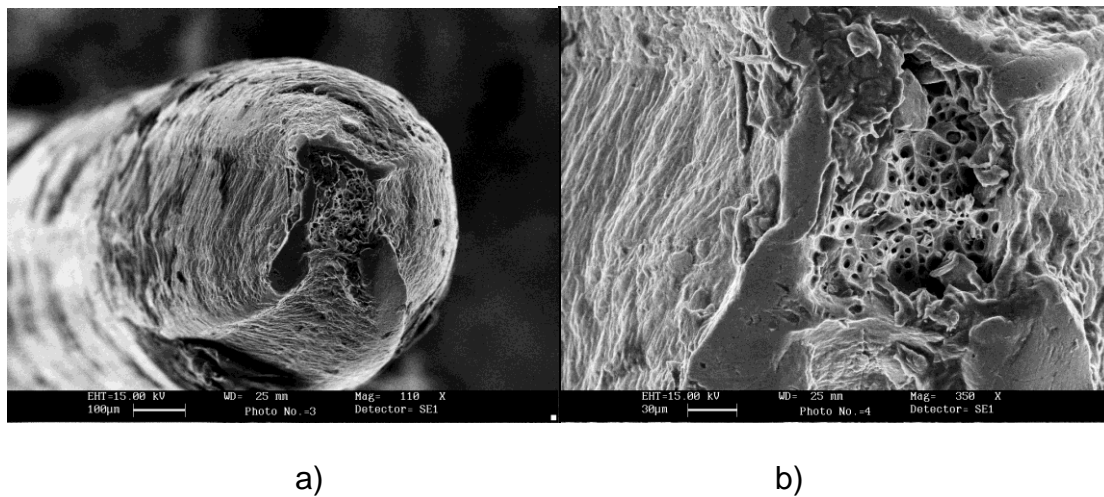
Fig. 20: SEM fractographs of the creep ruptured surface of aluminium wire a) low magnification showing significant reduction in cross section and b) high magnification showing dimple

5. SUMMARY

An algorithm has been presented for computing the probability of occurrence of inrush current greater than threshold value and loss of life of DTs due to inrush current and CLPU. The life of the low rating DTs are found to be more affected by the inrush current compared to the high rating DTs. With the increase in the KVA rating of DTs, the effect of the inrush current reduces because of the nearly same residual flux for all ratings DTs. The creep behavior of aluminum is very poor in comparison to copper. The use aluminum conductor for DTs subjected to frequent switching is not recommended;

however for low loss transformers aluminum conductor may be used with lower current density (say <1.1 A/mm^2).

The CLPU is another severe problem for Indian environment with increasing thermostatically controlled load. It causes accelerated degradation of winding insulation. This is more severe for small DTs having lower thermal time constant. To overcome CLPU problem a proper restoration scheme [7] along with higher capacity DTs are to be used. Further investigations from field data and experimental results will be of great help for optimal strategies that may reduce the failure of the transformers.

6.   CREEP RESULTS OF ALUMINUM AND COPPER WIRE WITH DISCUSSION

The CLPU current produces high stress and temperature in the windings of DTs. The frequent switching of DTs increases the probability that winding conductors may be operated at the stress between 1.24 to 6.64 kg/mm^2 and temperature well above the ambient temperature i.e., hot spot temperature which is 100 °C or in some cases 140 °C. The stress and hot spot temperature are calculated as per loading profile given in IS 6600:1972. The time constant of DTs windings is very low around 10 minutes. Thus, the temperature rise in the windings is very fast. These conditions of stress and temperature during frequent energization of DTs are sufficient for elongation of the winding conductors due to creep. The elongation causes loosening of the winding conductors between spacers. If elongation or strain in the wire is more than the allowable gap between two layers of the winding then turn to turn fault occurs. Thus, DTs are failed due to creep of the winding conductor.

Creep phenomenon is a typical plastic deformation of crystalline solids at higher temperatures. At temperature above 0.4 T_m, the diffusion is predominant and so can stimulate the plastic deformation. Deformation due to diffusion takes place through the dislocation sliding and climbing. Also, diffusion can heal the deformed microstructures. Therefore, deformation process is homogeneous as the viscous medium. Generally, the homogeneous deformation is known as steady state creep behaviour for a wide strain range. Hence, the steady state region is a large part of the creep life of the material at high temperature. At lower temperatures, the effect of diffusion on creep behaviour of crystalline solids is negligible but the work hardening is more matter at the initial stage of plastic deformation.

The creep curve for aluminum wire at 100 °C and stress 1.24 kg/mm^2 is shown in Fig. 21. At this condition, the steady state creep rate is obtained approximately as 1.96x10-04 mm/mm/hour. The creep curve for aluminum wire at 100 °C and 6.64 kg/mm^2 is shown in Fig. 22. At this condition, the steady state creep rate is computed approximately as 26.04x10^{-04} mm/mm/hour. The creep curve for aluminum wire at 140 °C and 4 kg/mm^2 is shown in Fig. 23. At this condition, the steady state creep rate is found approximately as 25.54x10^{-04} mm/mm/hour. The creep curve for aluminum wire at 140 °C and 6.64 kg/mm^2

is shown in Fig. 24. At this condition, the steady state creep rate is obtained approximately as 44.68x10^{-04} mm/mm/hour.

Table 9: Steady State Creep Rate of Aluminum and Copper Wire

S. No.	Type of Wire	Temp. (˚C)	Stress (kg/mm^2)	Steady State Creep Rate (mm/mm/hour)
1.	Aluminum	100	1.24	1.96x10^{-04}
2.	Aluminum	100	6.64	26.04 x10^{-04}
3.	Aluminum	140	4	25.54x10^{-04}
4.	Aluminum	140	6.64	44.68x10^{-04}
5.	Copper	140	4	1.18x10^{-04}
6.	Copper	140	6.64	1.79x10^{-04}

The steady state creep stage has not been examined for copper at 100 ˚C and 6.64 kg/mm^2. The creep curve for copper wire at 140 ˚C and 4 kg/mm^2 is shown in Figure 25. At this condition, the steady state creep rate is obtained as 1.18x10^{-04} mm/mm/hour. The creep curve for copper wire at 140 ˚C and 6.64 kg/mm^2 is shown in Fig. 26. At this condition, the steady state creep rate is obtained as 1.79x10^{-04} mm/mm/hour [11]. The steady state creep rates for all the conditions described above are summarized in Table 9.
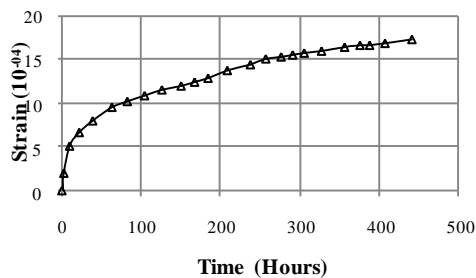

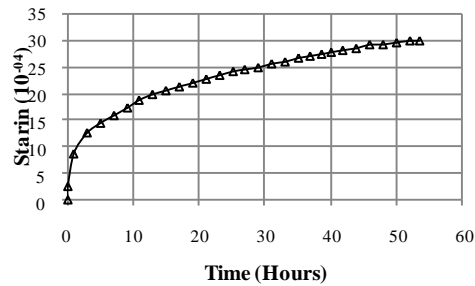Fig. 21: Creep Curve for Aluminum wire of Dia. 0.8 mm at 100 ˚C and 1.24 kg/mm^2

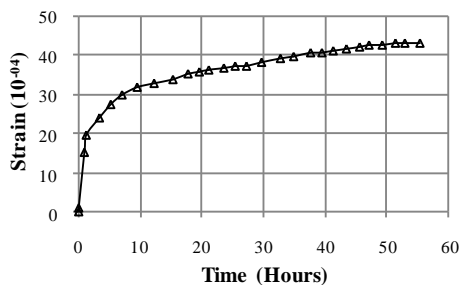Fig. 22: Creep Curve for Aluminum Wire of Dia. 0.8 mm at 100 ˚C and 6.64 kg/mm^2

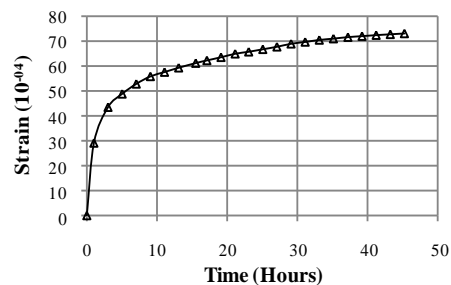Fig. 23: Creep Curve for Aluminum Wire of Dia. 0.8 mm at 140 ˚C and 4 kg/mm^2

Fig. 24: Creep Curve for Aluminum Wire of Dia. 0.8 mm at 140 ˚C and 6.64 kg/mm^2
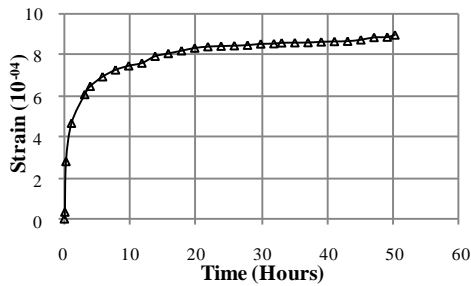
Fig. 25: Creep Curve for Copper Wire of Dia. 0.62 mm at 140 °C and 4 kg/mm^2
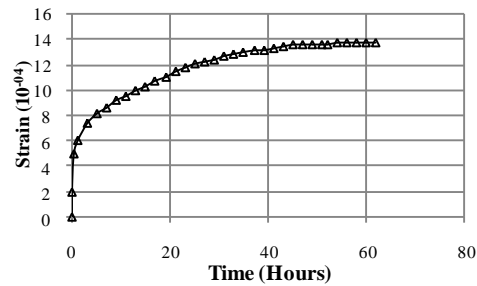

Fig. 26: Creep Curve for Copper Wire of Dia. 0.62 mm at 140 °C and 6.64 kg/mm^2

The effect of temperature, applied stress and material on steady state creep rate and time required for turn to turn fault due to creep are discussed as follows:

6.1 THE EFFECT OF TEMPERATURE

The effect of temperature is drastic and critical on the creep behaviour of aluminum and copper wire. The diffusion is active and important in these experimental conditions whereas recrystallization is not recognized. The diffusion would accelerate the plastic deformation and result in shortened rupture. For aluminum wire at 6.64 kg/mm^2, the steady state creep rate and time required for turn to turn fault at 140 °C are approximately 1.7 and 0.32 times, respectively than at 100 °C. Hence, DTs are failed earlier at higher operating temperature conditions.

6.2 THE EFFECT OF APPLIED STRESS

The creep curve depends upon the applied stress. As the applied stress increases, the creep curve changes from a logarithmic creep to a steady state creep. For aluminum wire at 100 °C, the steady state creep rate and time required for turn to turn fault at 6.64 kg/mm^2 are approximately 13.3 and 0.1 times, respectively than at 1.24 kg/mm^2. For aluminum wire at 140 °C, the steady state creep rate and turn to turn fault at 6.64 kg/mm^2 are 1.75 and 0.4 times, respectively than at 4 kg/mm^2. At 140 °C, the steady state creep rate and time for turn to turn fault for copper wire at 6.64 kg/mm^2 are around 1.51 and 0.11 times, respectively than at 4 kg/mm^2. Hence, DTs are failed earlier at higher stress. A survey has also been performed on about 100 damaged HT windings of aluminum and copper wound DTs and it is observed that 70% of the windings are damaged from their inner side. This fact suggests that stress developed in the HT windings due to CLPU current is highest on their inner side.

6.3 THE EFFECT OF MATERIAL

The creep curve depends extremely on the material. The steady state creep rates of aluminum wire at 140 °C corresponding to 4 and 6.64 kg/mm^2 are 21.64 and 24.96 times, respectively than copper wire. At 140 °C, the time required for turn to turn fault at 4 and 6.64 kg/mm^2 for aluminum wire is approximately 0.03 and 0.01 times, respectively than for copper wire. This fact suggests higher failure of aluminum wound DTs than copper wound DTs in the same operating conditions. Data have been collected for failure rate of

DTs and it is found that failure rate of aluminum wound DTs is 30% more than copper wound DTs.

7. FIELD CASE STUDY

The HT coils of failed DTs collected from the field also indicate high failure rate near inner layer and in the vicinity of HST. About 65% failure of HT coils are may be due to the reasons stated above i.e., poor creep behaviour of aluminum and frequent switching of DTs. The photographs of failed coils taken from field are shown in Fig. 27 -36.

8. CONCLUSIONS AND RECOMMENDATIONS

This report presents the experimental results of steady state creep rate and time required for turn to turn fault of aluminum and copper wires of diameter 0.8 and 0.62 mm, respectively at different temperature and stress conditions. The effect of temperature, stress and material on steady state creep rate is also studied. The temperatures for tests are taken 100 and 140 °C corresponding to the hot spot temperature in the HT winding of DTs. The stresses for tests are taken corresponding to the stress produced due to CLPU current on inner side of HT winding of DTs. For aluminum wire, the steady state creep rate and time for turn to turn fault at 140 °C are found approximately 1.7 and 0.32 times, respectively than at 100 °C, at same stress 6.64 kg/mm^2. For aluminum wire at 100 °C, the steady state creep rate and time for turn to turn fault at 6.64 kg/mm^2 are determined approximately 13.3 and 0.1 times than at 1.24 kg/mm^2. For aluminum wire at 140 °C, the steady state creep rate and time for turn to turn fault at 6.64 kg/mm^2 are obtained approximately 1.75 and 0.4 times, respectively than at 4 kg/mm^2. For copper wire at the temperature 140 °C, the steady state creep rate and time for turn to turn fault at 6.64 kg/mm^2 are approximately 1.51 and 0.11 times, respectively than at 4 kg/mm^2. At 140 °C, the steady state creep rate corresponding to 4 and 6.64 kg/mm^2 are respectively about 21.64 and 24.96 times more for aluminum wire than copper wire. The turn to turn fault time for aluminum wire at 4 and 6.64 kg/mm^2 are approximately 0.03 and 0.01 times, respectively than for copper wire at 140 °C.

The proposed study substantiates that the creep is the reason of DTs failure especially in power deficient areas and poor power distribution networks where frequent energization of DTs is required. DTs are failed earlier at high temperature and stress conditions due to CLPU current during their frequent energization. Also, the failure rate of aluminum wound DTs is more than copper wound DTs due to elevated steady state creep rate of aluminum wire than copper wire. To reduce the failure rate and the subsequent repairs of DTs, it is recommended to copper winding to ensure reliability.

Fig. 27. HT Coil damaged near to inner side

Fig. 28. HT Coil damaged maximum from inner side and transfer to outer side

Fig. 29. HT Coil damaged from inner side and almost center of coil height

Fig. 30. HT Coil damaged maximum from inner side

Fig. 31. HT coil heavily damaged from inner side

Fig. 32. HT coil deformed badly and damaged from inner side

Fig. 33. HT coil deformed badly from inner side

Fig. 34. HT coil damaged heavily from inner side

Fig. 35. HT coil damaged maximum on inner side

Fig. 36. HT coil damaged on top and maximum from inner side

Fig. 37. HT coil deformed badly and punctured at miidle of the coil width

Fig. 38. HT coil damaged badly from inner side

References

[1]. Rengarajan, S., et al., "Behaviour of High Voltage Machine Insulation System in the Presence of Thermal & Electrical Stresses," *IEEE Trans. on Electrical Insulation*, vol. E1-20, no. 1 Feb. 1985.

[2]. Ramu, T.S., "On the Estimation of Life of Power Apparatus Insulation under Combined Electrical & Thermal Stresses", *IEEE Trans. on Electrical Insulation*, vol. E1-20, no. 1, Feb. 1985.

[3]. Desai, B.T., Nair, N.C., and Gupta, H.O., "Inconsistency In Standards For Exact On Line Over Load Time-Limit Computation Based On Hot Spot Temperature Insulation Deterioration", *IEEMA Journal*, pp. 27-32, July 1993.

[4]. Michael Steurer and Klaus Frohlich, "The Impact of Inrush Currents on the Mechanical Stress of High Voltage Power Transformer Coils", *IEEE Transactions on Power Delivery*, vol. 17, no. 1, Jan 2002.

[5]. Laszlo Prikler, Gyorgy Banfai, Gabor Ban, Peter Becker, " Reducing the magnetizing inrush current by means of controlled energization and de-energization of large power transformers", *Electric Power Systems Research*, no.76, pp 642-649, 2006.

[6]. Ramsis Girgis, Ed teNyenhuis, "Characteristics of Inrush Current of Present Designs of Power Transformers", *IEEE Power Engineering Society General Meeting*, pp. 1-6, June 2007.

[7]. Kumar, Vishal, "Power Distribution System Operation under Cold Load Pickup", Ph.D thesis, Department of Electric Engineering, Indian Institute of Technology, Roorkee, India, Dec. 2006.

[8]. Gupta, H.O, "Transformer Reliability", *Electrical India*, vol. 47, pp. 118-123, Aug. 2007.

[9]. Gupta H.O., "Design and Manufacturing of Reliable Distribution Transformers," CBIP Seminar on Distribution Transformers Failures and New Developments, Lucknow, Feb. 6-7, 1997.

[10]. Beniwal N. S., Gupta, H. O., and Dwivedi D.K., "Effect of Creep on Reliability of Distribution Transformers," *National System Conference,* Indian Institute of Technology Roorkee, pp. 623-627, Dec. 17-19, 2008.

[11]. Beniwal N. S., Gupta, H. O., and Dwivedi D.K., "Effect of Creep on Failure Of Distribution Transformers-An Experimental Evaluation," *International Journal of Performability Engineering,* Accepted for publication in May 2010.

Appendix

Transformer Data	Core design parameters
Rated Power:100kVA No Load voltage: 11000/433 Mean dia (mm): 213.25 No of turns:3344 DC load loss (W):920	flux Densilty B_m(T): 1.685 B_{res}=0 to .83 of B_m B_{sat}=1.125*B_m Core Dia(mm): 110.909 Window height (mm):470
Rated Power:63kVA No Load voltage: 11000/433 Mean dia (mm): 195 No of turns:4356 DC load loss (W):640	flux Densilty B_m(T): 1.69 Core Dia(mm): 97.1288 Window height (mm):445
Rated Power:25kVA No Load voltage: 11000/433 Mean dia (mm):160 No of turns:7216 DC load loss (W):377 Conductor Diameter: 0.8 mm (Aluminum Wound DTs) 　　　　　　0.62 mm (Copper Wound DTs)	flux Densilty B_m(T): 1.647 Core Dia(mm):76.8505 Window height (mm):405
Rated Power:25kVA No Load voltage: 11000/433 Mean dia (mm):159.25 No of turns:7304 DC load loss (W):380 Conductor Diameter: 0.8 mm (Aluminum Wound DTs) 　　　　　　0.62 mm (Copper Wound DTs)	flux Densilty B_m(T): 1.585 Core Dia(mm):77.7817 Window height (mm):380